On the coupling between the neutral upper atmosphere, ionosphere and inner magnetosphere

P. Bencze[1], E. Illés-Almár[2], J. Verő[1]

(1) Geodetic and Geophysical Research Institute, Hungarian Academy of Sciences, H-9401 Sopron, P.O.B. 5. Hungary. E-mail: bencze@ggki.hu

(2) Konkoly Observatory, Hungarian Academy of Sciences, H-1525 Budapest, P.O.B. 67. Hungary. E-mail: illés@konkoly.hu

Abstract. Coupling between the neutral upper atmosphere, ionosphere and inner magnetosphere has been studied considering north-south asymmetry of the neutral total density, seasonal and annual anomalies of the electron density in the F region, as well as the plasma exchange between the ionosphere and plasmasphere (inner magnetosphere). As indicator of the latter process geomagnetic pulsations have been used. Energy deposition by particle precipitation generating SAR arc radiation, post storm effect in the lower ionosphere and effects of energetic neutral atoms are also discussed. It has been found that neutral density and temperature are enhanced in the whole year, but primely in winter as compared to the same season in the southern hemisphere. Electron density indicates the same behaviour due to the increased electron density gradient and increase of ambipolar diffusion in the F region. Excessive heating in the northern hemisphere as compared with the southern hemisphere may be due to excessive electron precipitation from the radiation belts, as well as from the ring current in subauroral latitudes and to energetic neutral atoms related to enhanced neutral density at low and middle latitudes. Estimates of energy deposition are given.

Keywords. Neutral upper atmosphere (Thermosphere) – Ionosphere (F-region) – Magnetosphere (Plasmasphere).

1 Introduction

If we will characterize simply the space around the Earth extending to the magnetopause, it can be devided into two regions. In the first region there is a close coupling between the neutral atmosphere and the ionosphere. In the second region this coupling is followed by a coupling between the ionized medium (plasmasphere, inner magnetosphere) and the geomagnetic field. Concerning relation of the ionosphere to the neutral atmosphere, it is not only composition of the neutral gas, which determines the initial ion composition. In the lower ionosphere motion of the neutral gas plays also an important role (dynamo region). Other coupling process between the neutral atmosphere and the ionosphere becomes predominant in the upper ionosphere, it is the composition change of the neutral atmosphere both in geomagnetically quiet and disturbed conditions. A coupling process of quite other kind occurs between the ionosphere and the inner magnetosphere due to the exchange of plasma, as well as particle precipitation originating in the radiation belts and the ring current.

2 Data and analysis

In Fig. 1 change of the total neutral density is shown as a function of latitude for both hemispheres. It can be seen that the density is higher in the northern hemisphere than in the southern hemisphere, that is, there is a density asymmetry between the northern and southern

thermosphere on the density of atomic oxygen, ion production decreases in this height region (above the F1 layer representing the altitude of maximum ionization) with altitude.

Concerning recombination, linear or β type recombination is the predominant process. Its magnitude is determined by the $[N_2]$ / $[O]$ ratio, as the rate of β type recombination is determined by the reaction $O + N_2 \rightarrow NO^+ + N$ (Rishbth et al., 2000; Zou et al., 2000). According to our calculations using atmospheric and ionospheric models, the rate of recombination at an altitude of 300 km and for an exospheric temperature of 1100 K attains a value of about $2.7 \cdot 10^7$ $m^{-3}s^{-1}$ (altitude and neutral temperature were selected taking that altitude and neutral temperature in the models, which correspond to the total neutral density asymmetry of $\Delta\rho/\rho \sim 0.2$). Concerning the effect of temperature change of about 94 K connected with the density increase of $\Delta\rho/\rho \sim 0.2$, $[N_2]$ / $[O]$ ratio increaes only by 0.03 at 300 km due to this temperature increase. This is due to the growing dominance of $[O]$ in the composition of the upper atmosphere with increasing altitude.

As regards transport, the transport term in the continuity equation is $\upsilon_{ID} \cdot \partial n_i / \partial z$. According to our calculations using Equ. 1, velocity of the ambipolar diffusion increases with height beginning to grow at altitudes above 160 km rising to about 10 ms^{-1} at 250 km and 70 ms^{-1} at 350 km, taking into account conditions valid for an exospheric temperature of 1100 K. For the transport term a value of $7.3 \cdot 10^7$ m^{-3} s^{-1} has been obtained referring to 300 km. Thus, in the continuity equation the transport term may be the dominant factor in determination of the electron density. Concerning the temperature assymmetry (~94 K) corresponding to the neutral density asymmetry $(\Delta\rho/\rho \sim 0.2)$ electron density would be enhanced in northerm hemisphere winter by growing velocity of ambipolar diffusion as a result of enhanced negative vertical gradient of electron density and reduced positive vertical gradient of plasma temperature. Thus, ambipolar diffusion would contribute to development of the north-south asymmetry of electron density at altitudes above the maximum electron density (NM F2). Increase of the ambipolar diffusion coefficient due to decrease of the ion-neutral collision frequency may be neglected because of the collision frequency approaching a limiting value with rising altitude.

As it is known, there is an exchange of plasma between the ionosphere and the inner magnetosphere (Schunk and Nagy, 2000). This plasma exchange is limited to that part of the magnetosphere called plasmasphere, where magnetic lines of force are closed and the exchange process takes place along these field lines. This confinement is due to effect of the geomagnetic field on charged particles permitting only a helical motion along field lines and a longitudinal motion perpendicular to the field lines. Filling of the plasmasphere with charged particles is controlled by the ionosphere (Denton et al., 2004). The plasma exchange between the ionosphere and the plasmasphere has a diurnal course, plasma transport directed by day from the ionosphere to the plasmasphere, which turns by night. Intensity of the exchange depends on electron density in the F-region.

The state of the plasmasphere can be studied by geomagnetic pulsations. For this purpose FLR (Field Line Resonance) type pulsations are suitable. Origin of these pulsations are upstream waves due to ion-cyclotron instability arising, when protons backscattered from the bow shock interact with solar wind protons. Upstream waves entering the magnetosphere result in formation of FLR type pulsations of the geomagnetic field in that part of the magnetosphere, where magnetic field lines are closed. Conditions of the origin of these pulsations are correspondence of a period in the spectrum of upstream waves with the eigenperiod of a field line. Field-lines behave like a string fixed in their ends and hereby torsional oscillations occur due to upstream waves of the same period. Thus, the period of FLR type pulsations changes with geomagnetic latitude increasing with latitude, while other periods of upstream waves are not enhanced. The upstream origin of FLR type pulsations has

also been demonstrated by the study of measurements carried out by means of the fluxgate vector magnetometer on board of CHAMP (Heilig et al., 2006). The eigenperiod of a field line is

$$T = 2\int \frac{ds}{V_A} = 2\int \frac{(4\pi\rho)^{1/2}}{B} ds \qquad (2)$$

where V_A is the Alfven velocity, ds is an elementary part of the field line, ρ stands for the plasma density B denoting intensity of the geomagnetic field. This shows that eigenperiod of a field line depends not only on length of the field line causing increase of the eigenperiod with geomagnetic latitude, but it is also proportional to the plasma density. If plasma density is increased due to enhancement of plasma transport from the ionosphere, the eigenperiod increases, too. The mechanism works like a resonant system, like an oscillating (resonant) circuit eigenperiod of which increasing with enhanced ohmic resistance (loading). In the field line resonance process electron density corresponds to the resistance damping amplitude and changing the period of FLR type pulsations. Thus, if electron density increases due to the north-south asymmetry, period of FLR type pulsations is also enhanced, as it will be shown later.

3 Results and discussion

Concerning the north-south asymmetry of the total neutral density (Fig. 1), it is observed more or less in every month of the year (Illés-Almár and Almár, 2006). In the ionosphere a similar asymmetry can be found in the F region of the ionosphere corresponding in height to the thermosphere. The electron density is higher in the northern winter hemisphere, than in the same season in the southern hemisphere as a result of the superpositon of the winter (seasonal) anomaly and the December anomaly. It has formerly been shown that this asymmetry occurs only in the winter months (November, December, January) and therefore, it is called December anomaly. An investigation of data measured at several station pairs located approximately at the same latitude and longitude in the northern and southern hemispheres (Table 1) has indicated that the difference of foF2 (characterizing the maximum electron density in the F region) between the hemispheres includes the period from September to July mainly at mid-latitudes. Thus, north-south asymmetry of the electron density extends almost to the whole year similarly to the neutral density. Though, the latter establishment is based only on six station pairs it may be regarded as reliable the latitudinal variation of he difference characterized by similar features from months to months. This is shown in Figs. 2-4, where the southern hemisphere part of the curve is obtained by mirroring the northern hemisphere part as compared with the equatorial plane (Bencze et al., 2005). The magnitude of the asymmetry indicates maxima at low and subauroral latitudes.

As it has already been shown in Part 2, due to the north-south asymmetry of the neutral temperature electron density is determined by increasing plasma transport in the height region considered here as a result of enhanced negative vertical gradient of the electron density and decreased positive vertical gradient of the plasma temperature. Effect of recombination is of minor importance. Thus, the December (annual) anomaly in the F-region may be attributed to the temperature increase in the thermosphere of the northern hemisphere indicated by north-south asymmetry of the total neutral density. Hereby coupling is established between the thermosphere and the ionosphere increase of the electron density in the F-region resulting in enhanced plasma transport from the ionosphere to the plasmasphere.

hemispheres (Illés-Almár and Almár, 2006). This Figure has been constructed with density values obtained by observing the drag of satellites. The density values were observed at different latitudes (inclination of the satellites 5°-96°) and longitudes, and they represent various altitudes (175-420 km) in the thermosphere. Measurements included both geomagnetically quiet and disturbed conditions(Almár et al., 1992). Data refer to different hours of the day and to different months.This variation of the density with latitude in both hemispheres plotted in Fig. 1 shows up in every month of the year. In this case the Figure represents a global average change, the tendency of which indicating enhanced density in the northern hemisphere as compared with the southern hemisphere. The relative density enhancement $[(\rho_{obs} - \rho_{CIRA}) / \rho_{CIRA} = \Delta\rho / \rho]$ attains a value of ~ 0.2 at high mid-latitudes.

In the thermosphere the neutral density is in winter months higher than in summer months. Thus, in the northern hemisphere density enhancements related to the north-south asymmetry and to the seasonal variation are superposed in winter. The situation is similar to that occurring in the F2 region (200-600 km) of the ionosphere, where in the northern hemisphere effects of the winter (seasonal) anomaly and the so called December (annual) anomaly are superposed.

It is emphasized that study of the electron density refers to the same height region as the neutral density data in Fig. 1. Consequently, inferring from the height region from which the mean value of neutral density changes are obtained the corresponding ionospheric region coincides to a large extent with the upper F2-region, with heights above the F2 layer maximum electron density. F2-region electron density is determined not only by linear (β type) recombination. In the height region in question effects of vertical transport processes are also important. As motion of charged particles is controlled by the geomagnetic field, they are moving along field lines. The process is called ambipolar diffusion and its veloity is given by the equation

$$v_D = -D_A \left(\frac{1}{n_i} \cdot \frac{\partial n_i}{\partial z} + \frac{1}{T_i} \cdot \frac{\partial T_p}{\partial z} - \frac{1}{H_p} \right) \cdot \cos I \qquad (1)$$

where $D_A = \dfrac{2kT_p}{m_i \nu_{in}}$ is the ambipolar diffusion coefficient. Here $T_p = (T_e + T_i)/2$ is the plasma temperature, k being Boltzmann's constant, T_e and T_i are the electron and the ion temperature, respectively, m_i is ion mass, ν_{in} stands for the ion-neutral collision frequency, n_i is the ion density, $H_p = kT_p / m_i g$ is the plasma scale height, I the dip angle. Our calculations carried out for different altitudes indicate that according to Equ. (1) v_D increases with increasing altitude in the height range above F2 maximum electron density determined by increasing negative trend of the vertical ion density gradients and decreasing positive trend of the vertical plasma temperature gradient (in a height region of about 300 km above the altitude of the F2 region maximum electron density). Besides D_A increasing also with altitude, the magnitude of the third term in the bracket enhances the value of v_D, that is $-1/H_p$ though it decreases with altitude. As a result, v_D is of positive sign in this region indicating an upward transport of charged particles.

Considering the continuity equation of charged particles, ion density changes depend on changes due to ionization, recombination and transport. If the mean value of changes must be determined as it has been done in case of the neutral density, diurnal and seasonal averages have to be used. Under these circumstances as a first approximation north-south asymmetry of ion-production can be neglected as compared with a possible asymmetry in recombination and transport. Though, ion production depends on the density of the ionizable gas – in the

Growth of the plasmaspheric electron density decreases activity of FLR type pulsations in consequence of damping of the resonance system by the enhanced electron density (Verő and Menk, 1986; Verő et al., 1995). The period of pulsations is also increased. The enhanced electron density in the plasmasphere causes reduced pulsation activity in the winter months. Spectra of geomagnetic pulsations show a peak around the local period of FLR type pulsations. This peak is of a width depending on the Q-factor of the resonant system. The Q-factor itself is inversely proportional to the ohmic resistance of the resonant circuit. Thus, if we accept the resonant circuit as an equivalent circuit, eigenperiod and width of the peak is determined by the electron density.

Geomagnetic pulsations are continuously recorded since 1957 in the Nagycenk Geophysical Observatory of the Geodetic and Geophysical Research Institute, Hungarian Academy of Sciences, Sopron (ϕ = 47.2°, Λ = 98,3°). Processed data are published in observatory reports of the Institute. In these reports occurrence frequency spectra of the recorded pulsations are also shown from 1957 to 1973 (Verő, 1961). Illustrations present mean occurrence frequency spectra of periods from about 1s to 10 min, each curve referring to an interval of 2 months of the year and the yearly mean is also given. Selected spectra are shown in Figs. 5-7, showing spectra characteristic of summer and winter months (Figs. 5-6) , as well as spectra indicating not only the occurrence frequency peak corresponding to FLR type pulsations, but also peaks belonging to other Pc type pulsations (Fig. 7). In these spectra generally two peaks can be seen, a greater one corresponding to the FLR type pulsations between 20 and 30s, as well as a much smaller one at about 2 min indicating Pi type pulsations. The latter are connected with geomagnetic substorms.

Occurrence frequency spectra can be characterized by three parameters, by their amplitude, by bandwidth and FLR period. Bandwith in case of an occurrence frequency spectrum means occurrence of other periods differing only slightly from eigenperiod of the field line. It may be regarded as a worsening of resonance conditions (damping). The amplitude of the occurrence frequency peak corresponding to FLR type pulsations shows increased values from 6h to 18h, that is, by day due to the source of their generation, namely upstream waves limited to the day side of the magnetosphere (Heilig et al., 2006). The bandwidth is enhanced by day due to electron density increase. The FLR period shows a similar behaviour indicating greater periods by day attributable to the same reason, as in case of the bandwidth. The seasonal variation of the occurrence frequency itself indicated an FLR peak, which is smaller in winter months (Fig. 6), than in summer months (Fig. 5) in accordance with winter-time enhancement of the elecron density in the ionosphere and transferred to the plasmasphere. Concerning the seasonal variation of bandwith and FLR period, occurrence frequency spectra indicate increasing bandwidth and growth of the FLR period in winter months (Fig. 6) as compared to summer months (Fig. 5) in accordance with the seasonal variation of electron density, however, only at high solar activity.

Taking values of the three parameters from the period 1969-1972, it has been found that occurrence frequency and bandwidth are correlated with solar activity significant at the 95 % level but only in case of winter months (November, December, January, February). Both parameters decrease with rising solar activity, however the change of the bandwidth with solar activity is very small. If the relation to geomagnetic activity is considered, the occurrence frequency is correlated with geomagnetic activity at the 95 % significance level, but only in that case, if all months are taken into account. Occurrence frequency increases with growing geomagnetic activity. Considering the bandwidth and the FLR period, both are correlated with geomagnetic activity at the 99 % significance level, but only in the winter months and are reduced with increasing geomagnetic activity. (Reduction of these parameters may be connected with observed electron density decrease of the ionosphere due to growing geomagnetic activity). This is a further proof of a coupling between the ionosphere and the

inner magnetosphere, which is further supported by CLUSTER observations indicating discret frequency field line resonances (FLRs) driven by magnetospheric waveguide modes (Mann et al. 2002). In situ CLUSTER measurements confirm the importance of ULF waves in magnetosphere-ionosphere coupling by generation and modulation of electron precipitation.

Coupling between the neutral upper atmosphere, the ionosphere and inner magnetosphere is also represented by particle precipitation of energetic particles from the radiation belts and the ring current resulting in heating, as well as ionization in the upper atmosphere and lower ionosphere, respectively(Bencze, 1991).

During geomagnetic disturbances, the cold high density plasma of the plasmasphere interact with the hot, thin plasma in the ring current. Thus, energy is transferred from ring current particles, in the majority of cases by high energy (> 10 keV) O^+ ions, to thermal electrons in the interaction region due to change exchange,Coulomb collision and wave-particle interactions (Kozyra et al., 1982; Kozyra et al., 1997; Schunk and Nagy, 2000). The energy originating in the ring current is conducted down along geomagnetic field lines into the ionosphere resulting in electron temperatures of 4000-10000 K (Wagner et al., 1986). Thus, at altitudes 300-400 km there are enough hot electrons (> 1.96 eV) in the tail of the thermal electron velocity distribution, which excite atomic oxygen from $O(^3P)$ to $O(^1D)$ state. Excited atoms emit radiation of 630 nm, the red line of atomic oxygen. The red line emission occurs in a latitudinally narrow region encircling the Earth at subauroral latitudes (45°- 55°). The phenomenon is called subauroral red (SAR) arc and contributes to heating of the high mid-latitude upper atmosphere (Fig. 8). [Enhanced electron temperatures not always high enough to produce SAR arc emissions are much more frequent and are characteristic of the subauroral ionosphere)].

Concerning diurnal variation of SAR arc in geomagnetically disturbed periods, they extend from the dusk to the dawn terminator as diffusive bands. Seasonal variation of SAR arc intensity has also been observed indicating winter maximum in the northern hemisphere (Slater and Smith, 1981). Increased intensity of SAR arcs in winter (electron temperature high enough) can be explained by enhanced heat flux, since increased heat flux can produce the same electron temperature in case of increased electron density (Coulomb collisions) (Kozyra et al., 1990). Enhanced heat flux can be the result of increased ring current O^+ density similar to O^+ density increase in the winter ionosphere. O^+ ions, predominant ions – with rising geomagnetic activity up to 9000 km in the polar region are produced by the solar EUV radiaton in the ionosphere. These ions are energized in this height range by parallel and perpendicular acceleration forming energetic ion outflow. The energetic O^+ ions originating in the polar wind (dominant source of H^+ ions), cleft ion fountain and the auroral zone get from the high latitude ionosphere into the inner plasma sheet, from where drifting earthward they are further energized and form the ring current (Huddleston et al. 2005).

This lengthy introduction to physical processes of SAR arc formation is thought to be necessary for discussion of a possible effect of the north-south asymmetry in the thermosphere and ionosphere on SAR arc formation. According to observations, thermospheric neutral density is enhanced in the northern hemisphere as compared with the southern hemisphere, finding also enhanced electron density in the northern hemisphere. SAR arcs are first of all related to geomagnetic activity (in recovery phase of geomagnetic storms). Neutral temperature increase within SAR arcs as compared with temperatures outside arcs is observed (Hernandez et al., 1982; Watanabe and Kim 1984) attaining a mean value of 100-200 K, which corresponds to a relative density increase of $\Delta\rho/\rho \sim 0.6$ at 500 km altitude. It might be assumed that this heating may also be a source of atmospheric waves in the thermosphere along a dusk to dawn zone at subauroral latitudes (Prasad and Furman, 1975). Considering larger neutral and electron densities in northern hemisphere winter corresponding to the north-south asymmetry, it would decrease the electron temperature in the topside

ionosphere as a result of enhanced electron-ion and electron-neutral cooling. This would result in reduced 630 nm column emission intensities in the northern hemisphere winter as compared to the same season in the southern hemisphere.

As it is known, the radiation belts are also located in that part of the magnetosphere where magnetic field lines are closed, that is, in the inner magnetosphere (Schulz and Lanzerotti, 1974). Electrons are lost in the inner zone mainly by coulomb scattering into the loss cone, since electrons are scattered more easily because of their smaller mass than to be slowed down (Imhof, 1968). The „slot" located between the inner and outer electron belts at L ~ 3 is a region of anomalously intense pitch-angle diffusion (it is systematically moving outward with declining solar activity). According to recent investigations (Selesnick et al., 2003; Selesnick et al., 2004), it has been found that pitch angle diffusion is related to electron scattering by whistler mode plasmaspheric hiss waves being the primary source of pitch angle diffusion. In the outer belt electron precipitation may principally occur during the acceleration process indicated by electron fluxes increasing with rising geomagnetic activity and lowering with energy (Hess, 1968). Acceleration itself may be related to violation of the integral adiabatic invariant I of the magnetic field, if the magnetic field at the particle's mirror point changes in a time short as compared to the bounce period. In this case, particles at their mirror points are submitted to Fermi acceleration, some particles meeting mirror points moving toward them, other mirror points moving away from them due to magnetic field perturbations. As statistically more approaching encounters occur resulting in a net energy gain, mirror points are continuosly lowered decreasing the pitch angle of the particle until it gets into the loss cone and is lost into the atmosphere.

Temporal and spatial distribution of electron pricipitation from the radiation belts is controlled also by azimuthal drift. Longitudinal variation of the particle loss is determined by azimuthal drift. The balance between drift and pitch angle diffusion determines the longitudinal electron distribution. Plasmaspheric hiss is the principal factor in the diffusion mechanism at high L values enhanced during the recovery phase, while whistlers in the plasmaspheric hiss frequency band participate in the process at low L values (Abel and Thorne, 1998). In low altitudes only the low energy electrons are strongly scattered in direction, thus, such electrons can easily scattered back out, if their mirror points are below the top of the atmosphere. High energy particles reach deep into the atmosphere before loosing enough energy to be scattered. In case of mirror points in the high altitude thin atmosphere, low energy electrons can be scattered deep into the atmosphere and lost, but high energy electrons mirror without scattering. Nevertheless, the rate of pitch angle diffusion is higher on the dayside than on the nightside occasionally by a factor of ~10 (Selesnick et al., 2003; Selesnick et al., 2004).

As coulomb scattering depends on ion density and electron temperature, and scattering of electrons by the neutral atmosphere is proportional to the neutral density and electron temperature, the loss of radiation belt electrons is also related to variation of the total neutral density. Thus, the north-south asymmetry of the total neutral density may result in ~ 20 % enhancement of the loss of radiation belt electrons in the northern hemisphere at mid and high latitudes.

In the outer belt electron precipitation can also be due to self-excited ion-cyclotron waves (Kennel and Petschek, 1966). The scattering process is resonant interaction between waves and particles, where the doppler shifted frequency of the former equals the gyrofrequency of the latter. Outer radiation belt electrons can also be affected by toroidal ULF waves (Ukhorskiy et al. 2005).

Precipitating electrons of energy > 40 keV originating in the „slot" region of the radiation belts produce the so called geomagnetic after effect, or post storm effect demonstrated by enhanced electron density in the lower ionosphere (Lauter and Knuth,

1967; Schulz and Lanzerotti, 1974, Peres, 1981, Märcz, 1986). Anomalous increase of the electron density appears 3-4 days after the primary ionization, when disturbances of the geomagnetic field ceased long ago. This after effect has been found to last up to 10 days after the storm (Fig. 9) and can be observed at geomagnetic latitudes greater than about 50° corresponding to that region of the radiation zones (L ~ 3), from where electron precipitation comes (slot region). An asymmetry in ionospheric absorption of radio waves in the lower ionosphere between the northern and southern midlatitudes has been found mostly in features of the winter anomly (Schwentek et al., 1980). This asymmetry is suggested to be due to different meteorological processes occuring in the two hemispheres in winter.

In the inner zone, protons are first slowed down by interacting with the atmosphere until their energy is reduced to about 100 keV. Longitudinal drift of these lower energy particles – besides protons also He^+ and O^+ ions form a ring of current encircling the Earth. Ring current characteristic thickness is within one ion gyroradius (62 km) (Roelof et al., 1985; Torr et al., 1982). Intensity of the ring current is increasing with geomagnetic activity reaching peak values during the main phase of geomagnetic storms. In the recovery phase of geomagnetic storms decrease of the ring current intensity is effected by charge exchange processes (Smith et al. 1981; Roelof, 1997). The energy of energetic ions incident in the atmosphere is almost entirely transferred to charge exchanged energetic neutral atoms (ENA), which afterwards propagate along nearly straight-line path (Vallat et al., 2004; DeMagistre et al., 2004). The ENA intensity originating in charge exchange consists of two parts. The first part is due to charge exchange between protons and hydrogen atoms in the exosphere producing slow protons and energetic neutral hydrogen atoms. The second part represents the ENA flux that is the result of charge exchange between ring current oxygen ions and hydrogen atoms creating slow protons and energetic neutral oxygen atoms at the exobase, a shell at an altitude of ~350 km. ENAs may be considered as the source of heating the cooling rate of energetic O^+ ions to neutrals being max. 5.10^{10} (Fig.10) (Torr et al., 1982). As a result of this heating anomalous density increase has been observed at low and low-middle latitudes (Prölss, 1982; Bencze and Illés-Almár, 1986; Bencze et al. 1993).

Density perturbations originating in the auroral zones due to their sudden thermal expansion propagate from high to low latitudes at both hemispheres crossing each other at the equator, as it has been observed by the STAR accelerometer on board of the CHAMP satellite (Forbes et al., 2005). Model calculations have indicated that the heating rate at low latitudes related to these atmospheric disturbances in geomagnetically disturbed periods is less than the energy deposition due to particle precipitation (Illés-Almár et al., 1996).

4 Conclusions

On the basis of discussion of the results, the following conclusions may be drawn up.

The north-south asymmetry observed in the total neutral density of the thermosphere hints at a temperature asymmetry with higher temperature in the northern hemisphere as compared to the southern hemisphere, remarking that the total neutral density originates practically only from atomic oxygen. Enhanced atomic oxygen in the northern hemisphere results in the observed increase of electron density in F-region of the ionosphere due mainly to enhanced upward plasmatransport (ambipolar diffusion) in the height region, where the north-south neutral density asymmetry has been found.

The eigen-period of FLR type geomagnetic pulsations depends on geomagnetic latitude, but also on plasmaspheric electron density, the latter being function of the ionospheric electron density. Thus, north-south asymmetry of the F region electron density can be observed in the activity of FLR type pulsations their occurrence strongly reduced in northern winter months and their eigenperiod increased.

During geomagnetic disturbances energy is transferred from the ring current to thermal electrons, the energy conducted dawn along geomagnetic field lines into the ionosphere at high mid-latitude resulting in heating and excitation of atomic oxygen (SAR arc formation).

Protons originating in the inner radiation zone produce energetic neutral atoms (ENA) due to multiple charge exchange contributing to heating of the thermosphere at low mid-latitudes as it has been observed.

Loss of radiation belt electrons contributes also to the energy exchange between the radiation belts and the atmosphere.

Electron precipitation from the „slot" region located between the inner and outer radiation zones is related to observed occurrence of the post storm effect in the lower ionosphere.

Thus, it is demonstrated that there is a manysided coupling between the thermosphere, the ionosphere and the inner magnetosphere (Amory-Mazaudier, 2006; Aruliah, 2006).

However, the main question remains as what may be the source of energy producing the temperature asymmetry indicated by north-south asymmetry of the neutral density. In our calculation presented below the CIRA 1986 atmospheric models and the IRI 1990 have been used. If the neutral density is higher in the northern hemisphere than in the southern hemisphere, the loss of radiation belt electrons would be enhanced in the northern hemisphere, which would attain about 20 %. The north-south asymmetry would increase the energy deposition in the subauroral SAR arc zone as a result of increased energy deposition. Calculations have shown that the energy deposition to electrons by electron cooling is approximately 10^{10} $eVm^{-3}s^{-1}$ (Fok et al., 1993). In case of enhanced electron density in northern hemisphere winter the cooling rate would be ~ $1.1 \cdot 10^{10}$ eV $m^{-3}s^{-1}$ at L = 2.5 on the nightside. The heating increase in the northern hemisphere due to the north-south asymmetry of the neutral density would amount to 1.10^{10} eV $m^{-3}s^{-1}$. Excessive energy deposition would result in the flux of energetic neutral atoms (O,H) at low and middle latitudes during the recovery phase of geomagnetic storms, which originate in the ring current (Illés-Almár, 2004). According to calculations, estimated value of the energy deposition, the cooling rate of energetic O^+ ions to neutrals is about 5.10^{10} $eVm\text{-}^3s^{-1}$ maximizing at about 350 km on the night side (Torr et al. 1982). Cooling decreases both below and above this altitude. Considering the neutral density asymmetry, a relative increase of 0.2 would enhance proportionally the ion-neutral cooling rate, since the momentum transfer collision frequency is proportional to the neutral density. Thus, the ion-neutral cooling rate would increase to about 6.10^{10} $eVm^{-3}s^{-1}$ at the height of the maximum energy deposition. The excessive heating related to ENA's in the northern hemisphere due to the north-south asymmetry of the neutral density would amount to 1.10^{10} $eVm^{-3}s^{-1}$. As a comparison, the solar UV/EUV energy deposition in 300 km altitude is about $5 \cdot 10^9$ eV $m^{-3}s^{-1}$ (Torr et al., 1980).

Acknowledgements. Authors acknowledge the financial support provided by the Hungarian Space Office in the grants TP 121 and TP 151. Thanks are due to Prof. I. Almár for useful discussions.

References

Abel, A., Thorne, R. M.: Electron scattering loss in the Earth's inner magnetosphere: 1. Dominant physical processes. J. Geophys. Res., 103, 2385-2396, 1998.

Almár, I., Illés-Almár, E., Horváth, A., Kolláth, Z., Bisikalo, D. V., Kasimenko, T. V.: Improvement of the MSIS-86 and DTM thermospheric models by investigating the geomagnetic effect. Adv. Space Res., 12(6), 313-316, 1992.

Amory-Mazaudier, C.: Some aspect of the coupling between ionosphere with neutral middle atmosphere and thermosphere. EGUO6-A-02899, 2006. augusztus 10.

Aruliah, A.L.: Thermospheric preconditioning of the ionosphere and response to geomagnetic activity. EGU06-A-06518, 2006.

Bencze, P., Almár, I., Illés-Almár, E.: North-south asymmetry in the thermosphere and ionosphere. EGU05-A-03078, 2005.

Bencze, P., Almár, I., Illés-Almár, E.: Ring current heating of the low latitude thermosphere connected with geomagnetic disturbances. Adv. space Res., 13, 303-306, 1993.

Bencze, P., Illés-Almár, E.: The flux of the ring current protons as an additional heat source for the neutral upper atmosphere after geomagnetic storms, in: Nabl.ISZ vol. 24, 121-127, 1986.

Bencze, P.: A joint view of geomagnetic, ionospheric and thermospheric disturbances. Acta Geod. Geoph. Mont. Hung., 26, 237-251, 1991.

CIRA 1972, Akademie Verlag, Berlin, 1972.

CIRA 1986 (ed. D. Rees). Pergamon Press, Oxford, 1989.

DeMagistre, R., Roelof, E. C., Brandt, P.C, Son, Mitchell, D. G.: Retrieval of global magnetospheric ion distributions from high-energy neutral atom measurements made by the IMAGE/HENA instrument. J. Geophys. Res., 109, A4, AO4214, 2004.

Denton, R. E., Menietti, J. D., Goldstein, J., Young, S. L., Anderson, R. R.: Electron density in the magnetosphere. J. Geophys. Res., 109, A09215, 2004.

Fok, M.-C., Kozyra, J. U., Nagy. A. F., Rasmussen, C. E., Khazanov, G. V.: Decay of equatorial ring current ions and associated aeronomical consequences. J. Geophys. Res., 98, 19, 381-393, 1993.

Forbes. J. M., Lu, G., Bruinsma, S., Nerem, S., Zhang, X.: Thermosphere density variations due to the 15-24 April 2002 solar events from CHAMP/STAR accelerometer measurements. J. Geophys. Res., 110, A12527, 2005.

Heilig, B., Lühr, H., Rother, M.. Statistical survey of compressional Pc 3 pulsations at low Earth orbit observed by CHAMP. EGU, 06-A-02513, 2006.

Hernandez, G., Meriwether, J. W., Tepley, C. A., Hays, P. B., Cogger, L. L., Slater, D. W., Roble, R. G., Emery, B. A., Evans, D. S.: Thermospheric response to the 23 October 1981 SAR arc and aurora as observed rom Fritz Peak, Colorado, and Calgary, Alberta during the Dynamic Explorer (DE-2) and NOAA-6 satellite overflights. Geophys. Res. Lett., 9, 969-972, 1982.

Hess, W. N.: The Radiation Belt and Magnetosphere. Blaisdell Publ. Co, Waltham, MA, USA, 1968.

Huddleston, M. M., Chappell, C. R., Delcourt, D. C., Moore, T. E., Giles, B. L., Chandler, M. O.: An examination of the process and magnitude of ionospheric plasma supply to the magnetosphere. J. Geophys. Res., 110, A12202 (2005).

Illés-Almár, E., Almár, I., Bencze, P.: Observational results hinting at the coupling of the thermosphere with the ionosphere/magnetosphere system and with the middle atmosphere. Adv. space Res., 18 (3), 45-48, 1996.

Illés-Almár, E., Almár, I.: A north-south asymmetry in thermospheric density (Submitted to Adv. Space Res.) 2006.

Illés-Almár, E.: Two distinct sources of magnetospheric heating in the atmosphere, the aurora and the ring current. Adv. Space Res., 34, 1773-1778, 2004.

Imhof. W. L.: Electron precipitation in radiation belts. J. Geophys. Res., 73, 4167-4184, 1968.

International Reference Ionosphere 1990 (ed. D. Bilitza) NSSDC. Greenbelt, Maryland, U.S.A., 1990.

Kennel, C. F., Petchek, H. E.: Limit on stably trapped particle fluxes. J. Geophys. Res., 71, 1-28, 1966.

Kozyra, J. U., Nagy, A. F., Slater, D. W.: High altitude energy source(s) for stable auroral red arcs. Rev. Geophys., 35, 155-190, 1997.

Kozyra, J. U., Valladares, C. E., Carlson, H. C., Buonsanto, M. J., Slater, D. W.: A theoretical study of the seasonal and solar cycle variations of Stable Aurora Red Ares. J. Geophys. Res., 95, 12, 219-234, 1990.

Kozyra, J. W., Cravens, T. E., Nagy, A. F.: Energetic O^+ precipitation. J. Geophys. Res., 87, 2481-2486, 1982.

Lauter, E., A., Knuth, R.: Precipitation of high energy particles into the upper atmosphere at medium latitudes after magnetic storms. J. Atm. Terr. Phys., 29, 411-417, 1967.

Mann, I., R., Voronkov, I., Dunlop, M., Donovan, E., Yeoman, T. K., Milling, D. K., Wild, J., Kauristie, K., Amm, O., Bale, S. D., Balogh, A., Viljanen, A., Opgenoorth, H. J.: Coordinated ground-based and Cluster observations of large amplitude global magnetospheric oscillations during a fast solar wind speed interval. Ann. Geophysicae, 20, 405-426, 2002.

Märcz, F.: Three phases of post-storm events in ionospheric absorption. Acta Geod. Geophys. Montanist. Hung., 21, 201-207, 1986.

Peres, M.: Storm after-effects observed at Ushuaia and Kerguelen. J. Atmos. Terr. Phys., 43, 1279-1283, 1981.

Prasad, S., S., Furman, D. R.: Atmospheric gravity waves: their effects on ionospheric temperature and composition. J. Atmos. Terr. Phys., 37, 17-30, 1975.

Prölss, G. W.: Perturbation of the low-latitude upper atmosphere during magnetic substorm activity. J. Geophys. Res., 87, 5260-5266, 1982.

Rishbeth, H., Müller-Vodarg, I. C. F., Zou, L., Fuller-Rowell, T. J., Millward, G. H., Moffet, R. J., Idenden, D. W., Aylward, A. D.: Annual and semiannual variations in the ionospheric F2-layer, II. Physical discussion. Ann. Geophysicae, 18, 945-956, 2000.

Roelof, E. C.: ENA emission from nearly-mirroring magnetospheric ions interacting with the exosphere. Adv. Space Res., 20 (3), 361-366, 1997.

Roelof, E. C., Mitchell, D. G., Villiams, D. J.: Energetic neutral atoms (~ keV) from the ring current, IMP 7/8 and ISEE-1. J. Geophys. Res., 90, 10991-11008, 1985.

Schulz, M., Lanzerotti, L. J.: Particle Diffusion in the Radiation Belts. Springer-Verlag, Berlin, 1974.

Schunk, R. W., Nagy, A. F.: Ionospheres-Physics, Plasma Physics, and Chemistry, Cambridge University Press, Cambridge, 2000.

Schwentek, H., Elling, W., Peres, M.: Asymmetry in the winter anomalous behaviour of absorption at midlatitudes in the northern and southern hemispheres. J. Atmos. Terr. Phys., 42, 545-552, 1980.

Selesnick, R. S., Blake, J. B., Mewaldt, R. A.: Atmospheric losses of radiation belt electrons. J. Geophys. Res., 108, A12, 1468, 2003.

Selesnick, R. S., Looper, M. A., Albert, J. M.: Low-altitude distribution of radiation belt electrons. J. Geophys. Res, 109, A11, 209, 2004.

Slater, D. W., Smith, L. L.: Modulation of stable auroral red (SAR) arc occurrence rates. J. Geophys. res., 86, 3669-3673, 1981.

Smith, P. H., Bewtra, N. K., Hoffman, R. A.: Inference of the ring current ion composition by means of charge exchange decay. J. Geophys. Res., 86, 3470-3480, 1981.

Torr, M. R., Richards, P. G., Torr, D. G.: A new determination of the ultraviolet heating efficiency of the thermosphere. J. Geophys. Res., 85, 6819-6826, 1980.

Torr, M. R., Torr, D. G., Roble, R. G., Ridley, E. C.: The dynamic response of the thermosphere to the energy influx resulting from energetic 0^+ ions. J. Geophys. Res., 87, 5290-5300, 1982.

Ukhorskiy, A. Y., Takahashi, K., Anderson, B. J., Korth, H.: Impact of toroidal VLF waves on the outer radiation belt electrons. J. Geophys. Res., 110, A10202, 2005.

Vallat, C. et al.: First comparisons of local ion measurements in the inner magnetosphere with energetic neutral atom image inversions: Cluster-CIS and IMAGE-HENA observations. J. Geophys. Res., 109, A4, AO4213, 2004.

Verő, J., Best, I., Vellante, M., Lühr, H., De Lauretis, M., Holló, L., Märcz, F. Strestik, J.: Relations of field line resonances and upstream waves and the winter attenuation of pulsations. Ann. Geophysicae, 13, 689-697, 1995.

Verő, J., Menk, F. W.: Damping of geomagnetic pulsations at high F2 layer electron concentrations. J. Atm. Terr. Phys., 48, 231-245, 1986.

Verő, J.: Ein Versuch zur Trennung der einzelnen Frequenzbänder der Erdstromvariationen. Geof. Pura Appl., 49, 83-118, 1961.

Wagner, Ch. U., Förster, M., Johanning, G.: Paper presented at the 26th COSPAR Scientific Assembly, Toulouse, 1986.

Watanabe, T., Kim, J. S.: Photometric and interferometric observations of recent SAR arc events. J. Geomagn. Geoelectr., 36, 1-10, 1984.

Zou, L., Rishbeth, H., Müller-Vodarg, I. C. F., Aylward, A. D., Millward, G. H., Fuller-Rowell, T. J., Idenden, D. W., Moffet, R. J.: Annual and semiannul variations in the ionospheric F2-layer. I. Modelling. Ann.Geophysicae, 18, 927-944, 2000.

Figure captions

Fig. 1: Change of the total neutral density deviations from the CIRA 72 model values expressed by ($\rho_{obs} - \rho_{model} / \rho_{model}$) as a function of latitude for both hemispheres shown by the drag of different satellites (Illés-Almár and Almár, 2006)

Fig. 2: Difference of foF2 in corresponding months of the same season between the northern and southern hemispheres for the interval September 1958 - July 1959.

Fig. 3: Difference of foF2 in corresponding months of the same season between the northern and southern hemispheres for December 1957 and January 1958.

Fig. 4: Difference of foF2 in corresponding months of the same season between the northern and southern hemispheres for April 1958 and May 1958.

Fig. 5: Occurrence frequency spectrum of geomagnetic pulsations determined on the basis of earth current records of the Nagycenk Geophysical Observatory, May-June, 1960

Fig. 6: Occurrence frequency spectrum of geomagnetic pulsations determined from earth current records of the Nagycenk Geophysical Observatory, Nov.-Dec. 1960.

Fig. 7: Occurrence frequency spectrum of geomagnetic pulsations determined from earth current records of the Nagycenk Geophysical Observatory showing peaks corresponding to Pc 2, Pc 3, Pc 4 and Pi 2 pulsations.

Fig. 8: Heating of the thermosphere by ring current particles appearing in electron temperature (T_e) (Wagner et al., 1986).

Fig. 9: Post storm effect (geomagnetic after effect) represented by anomalous increase of radio wave absorption measured by the A3 method at mid-latitudes in the lower ionosphere showing from top to bottom change of geomagnetic activity (ΣKp), of night-time excess absorption (ΔL_N) and sunset excess absorption (ΔL_{ss}) from 3 days before to 15 days after beginning of the geomagnetic disturbance (Märcz, 1986).

Fig. 10: Heating of the thermosphere by energetic neutral particles related to day-time solar electromagnetic radiation (dashed line) and to nightside energetic O^+ precipitation (full line), height variation of the heating rate deduced from measured density values (circles) and due to atmospheric disturbances propagating from the auroral zones obtained hy modelling (crosses) (Torr et al. 1982; Bencze et al., 1993).

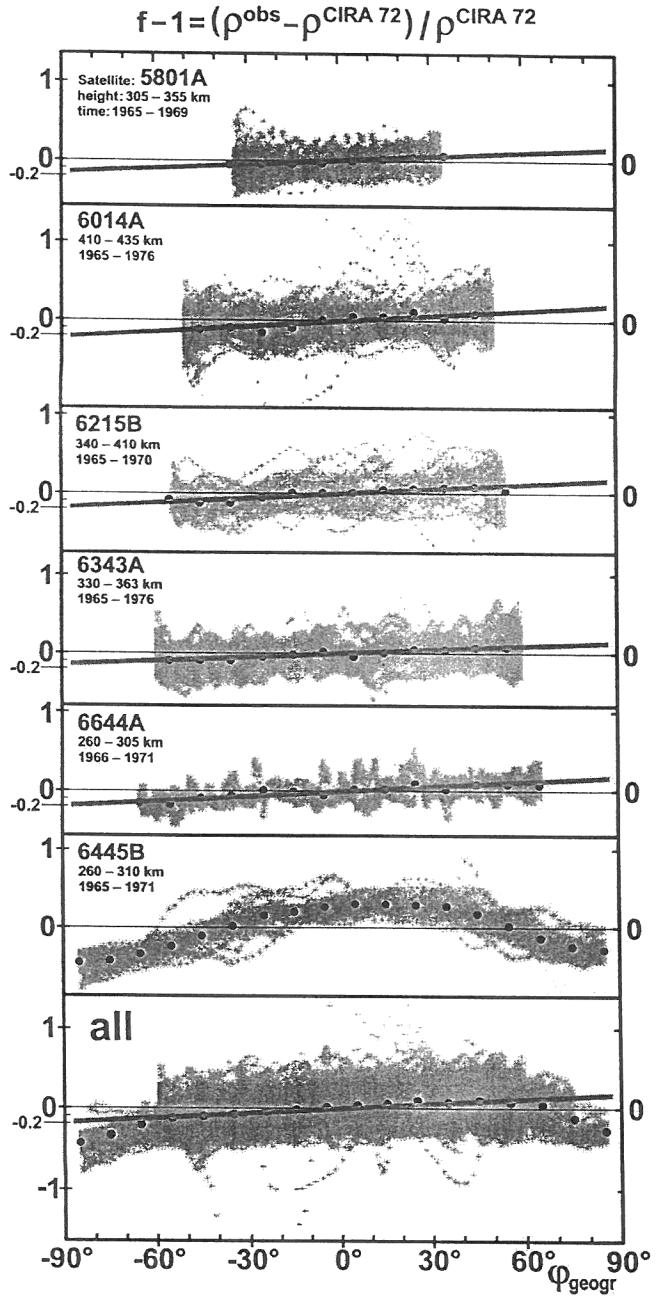
f−1=(ρobs−ρCIRA 72)/ρCIRA 72
Satellite: 5801A
height: 305 – 355 km
time: 1965 – 1969
6014A
410 – 435 km
1965 – 1976
6215B
340 – 410 km
1965 – 1970
6343A
330 – 363 km
1965 – 1976
6644A
260 – 305 km
1966 – 1971
6445B
260 – 310 km
1965 – 1971
all
-90° -60° -30° 0° 30° 60° 90°
φgeogr

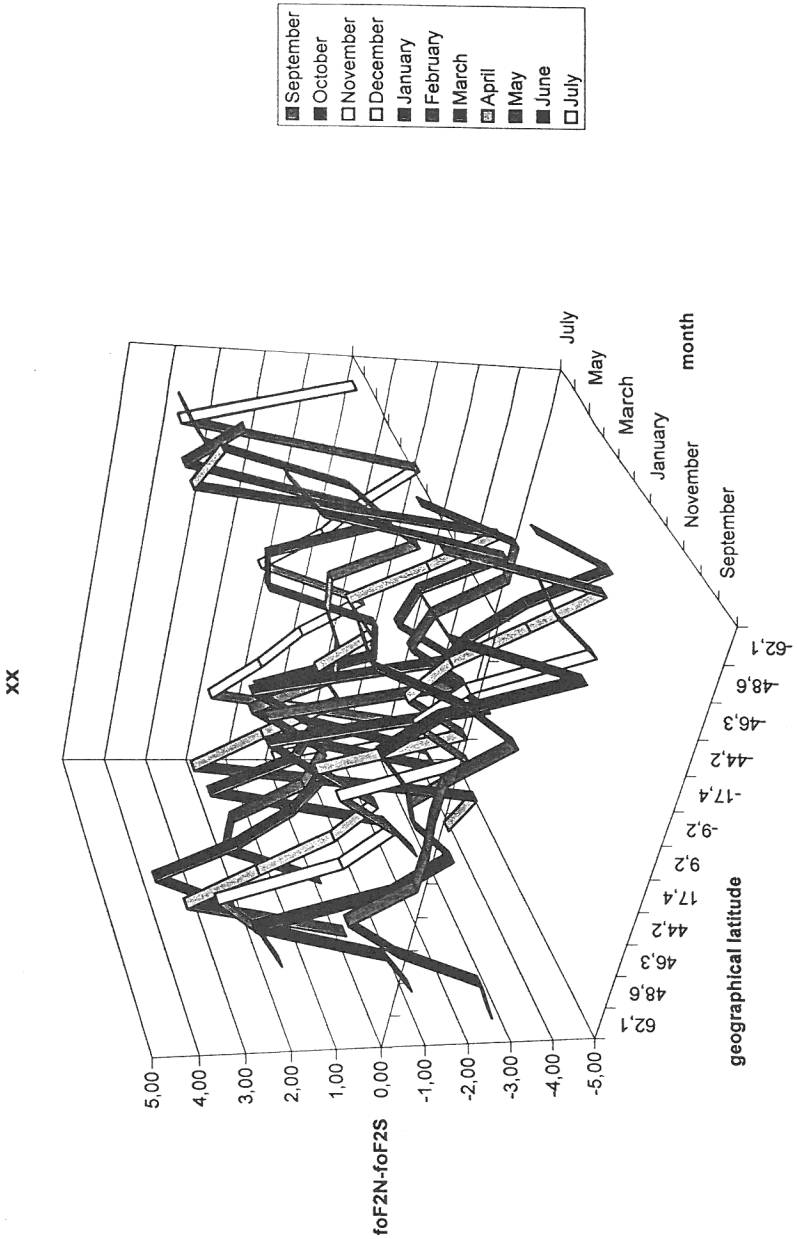
September
October
November
December
January
February
March
April
May
June
July
xx
July
May
March
January
November
September
month
62,1
48,6
46,3
44,2
17,4
9,2
-9,2
-17,4
-44,2
-46,3
-48,6
-62,1
geographical latitude
5,00
4,00
3,00
2,00
1,00
0,00
-1,00
-2,00
-3,00
-4,00
-5,00
foF2N-foF2S

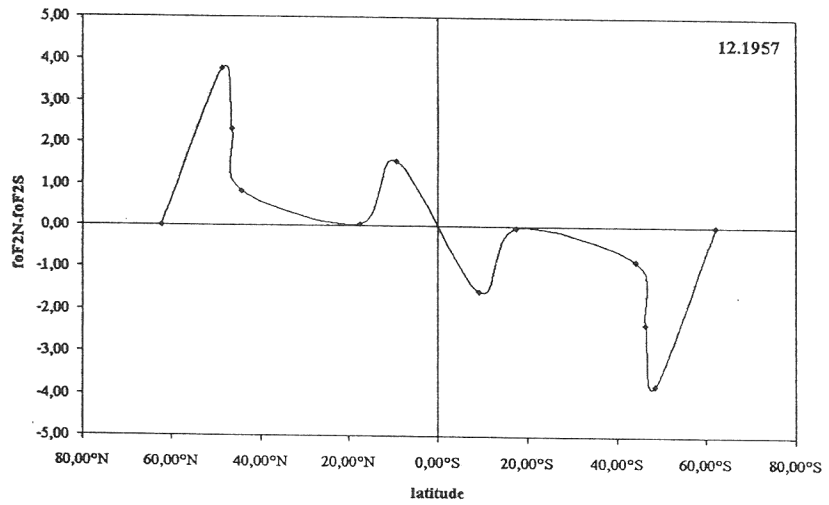
12.1957
foF2N-foF2S
5,00
4,00
3,00
2,00
1,00
0,00
-1,00
-2,00
-3,00
-4,00
-5,00
80,00°N
60,00°N
40,00°N
20,00°N
0,00°S
20,00°S
40,00°S
60,00°S
80,00°S
latitude

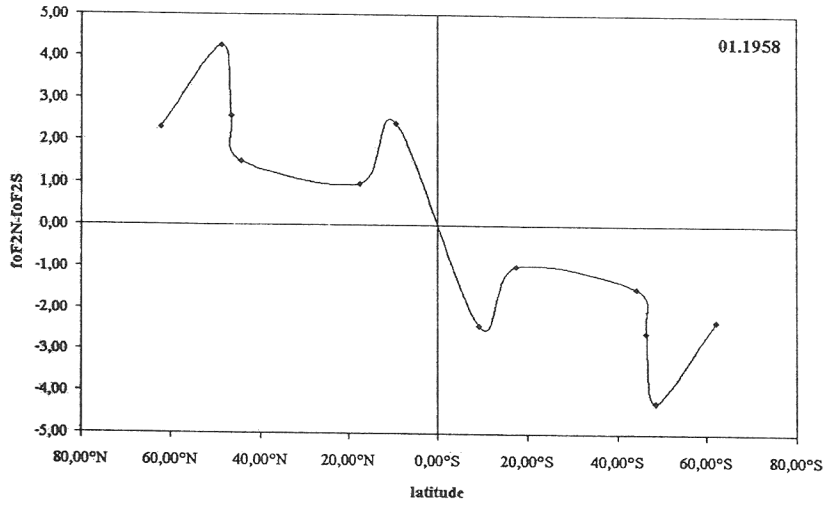
01.1958
foF2N-foF2S
5,00
4,00
3,00
2,00
1,00
0,00
-1,00
-2,00
-3,00
-4,00
-5,00
80,00°N
60,00°N
40,00°N
20,00°N
0,00°S
20,00°S
40,00°S
60,00°S
80,00°S
latitude

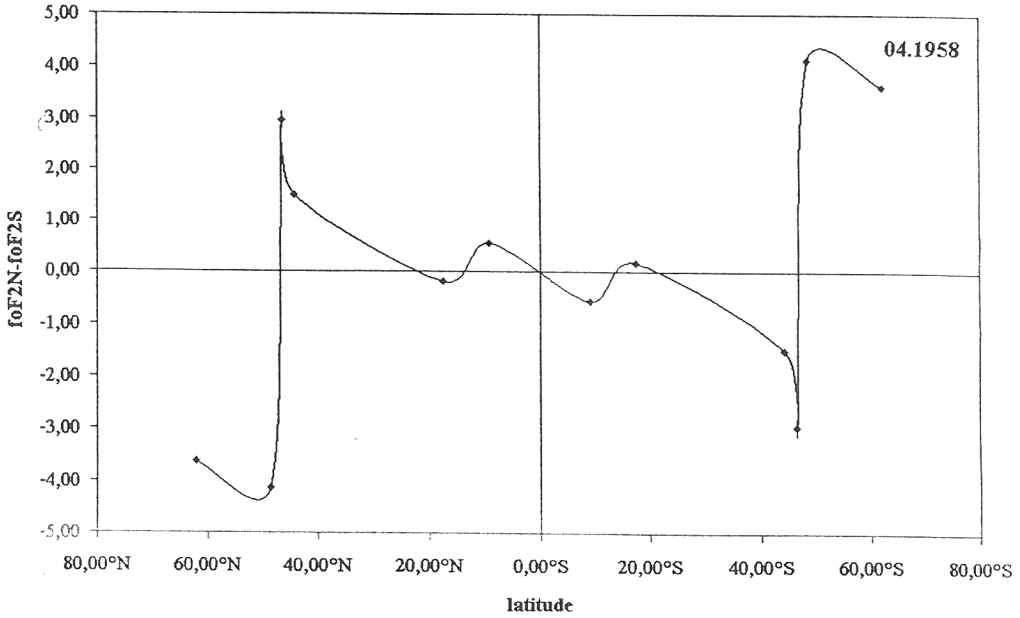
04.1958
foF2N-foF2S
5,00
4,00
3,00
2,00
1,00
0,00
-1,00
-2,00
-3,00
-4,00
-5,00
80,00°N
60,00°N
40,00°N
20,00°N
0,00°S
20,00°S
40,00°S
60,00°S
80,00°S
latitude

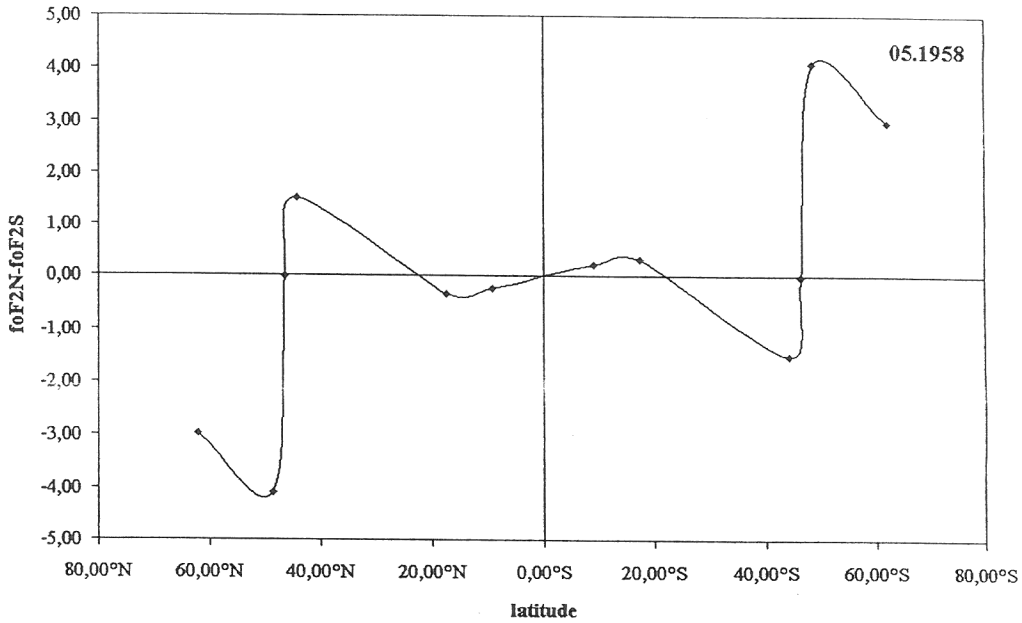
05.1958
foF2N-foF2S
5,00
4,00
3,00
2,00
1,00
0,00
-1,00
-2,00
-3,00
-4,00
-5,00
80,00°N
60,00°N
40,00°N
20,00°N
0,00°S
20,00°S
40,00°S
60,00°S
80,00°S
latitude

Fig 5

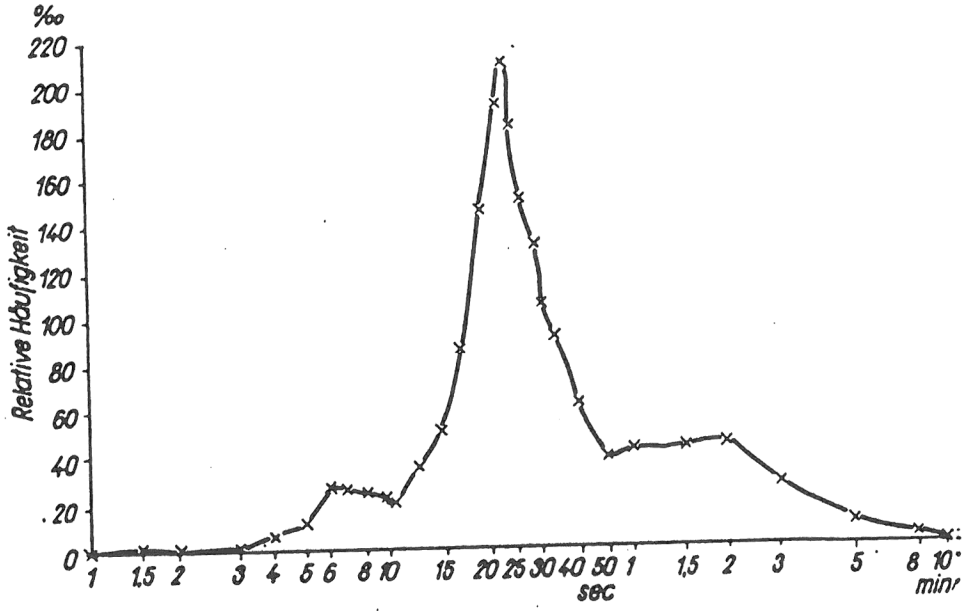
‰
220
200
180
160
140
120
100
80
60
40
20
0
Relative Häufigkeit
1 1,5 2 3 4 5 6 8 10 15 20 25 30 40 50 1 1,5 2 3 5 8 10
sec
min

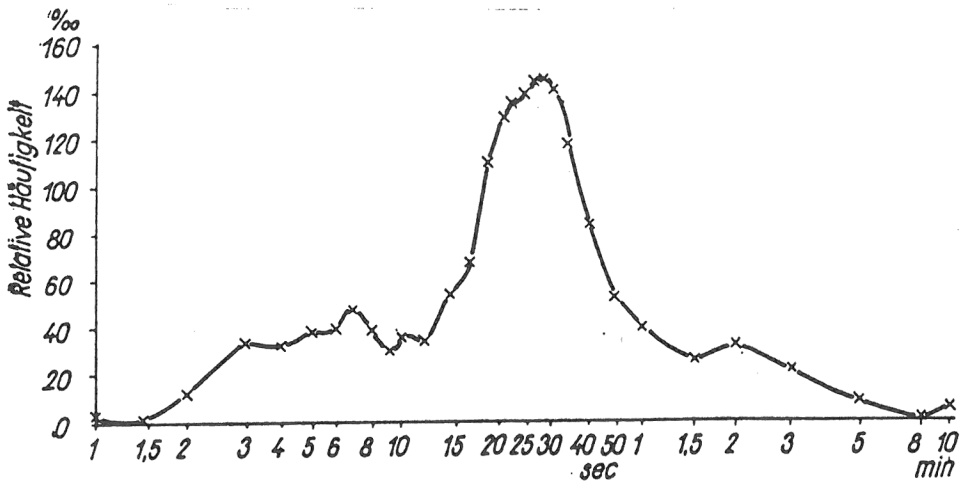
‰
160
140
120
100
80
60
40
20
0
Relative Häufigkeit
1 1,5 2 3 4 5 6 8 10 15 20 25 30 40 50 1 1,5 2 3 5 8 10
sec
min

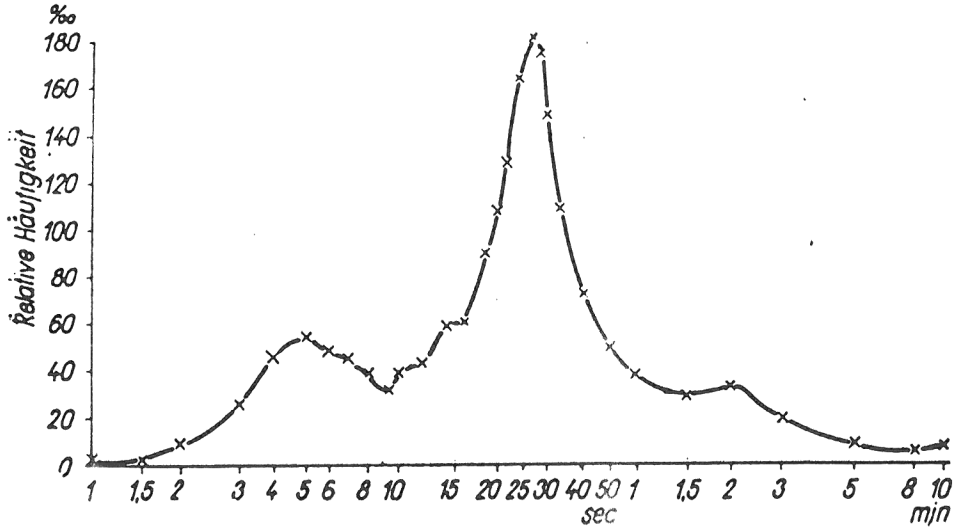
‰
180
160
140
120
100
80
60
40
20
0
Relative Häufigkeit
1 1,5 2 3 4 5 6 8 10 15 20 25 30 40 50
sec
1 1,5 2 3 5 8 10
min

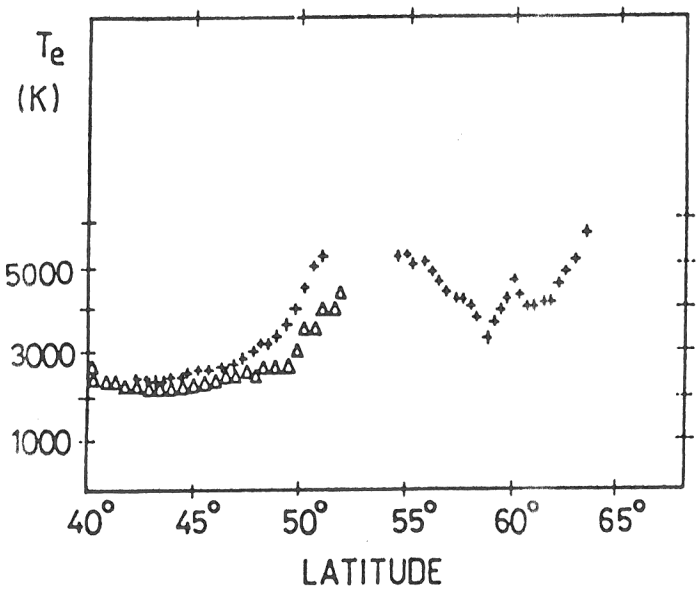
Te
(K)
5000
3000
1000
40° 45° 50° 55° 60° 65°
LATITUDE

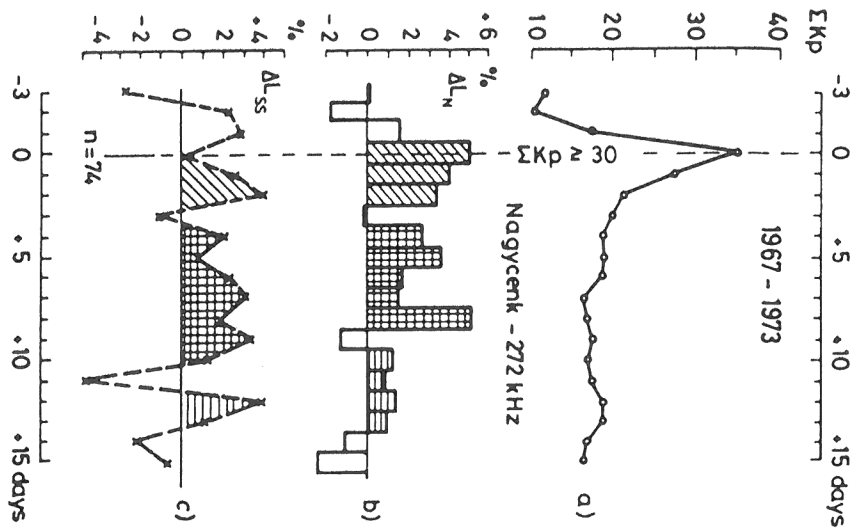
ΣKp
10
20
30
40
-3
0
+5
+10
+15 days
ΣKp ≥ 30
1967 - 1973
a)
Nagycenk - 272 kHz
%
-2
0
2
4
+6
ΔL_N
b)
n=74
%
-4
-2
0
2
+4
ΔL_SS
c)

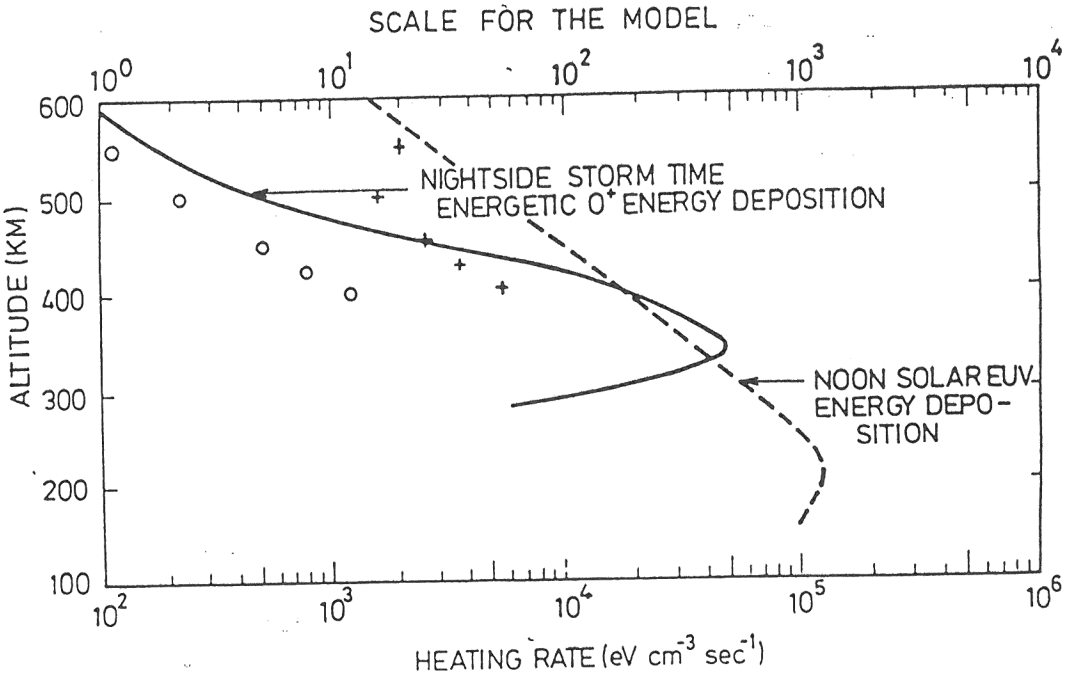
SCALE FOR THE MODEL
10^0
10^1
10^2
10^3
10^4
600
500
400
300
200
100
ALTITUDE (KM)
NIGHTSIDE STORM TIME
ENERGETIC O+ ENERGY DEPOSITION
NOON SOLAR EUV
ENERGY DEPO-
SITION
10^2
10^3
10^4
10^5
10^6
HEATING RATE (eV cm^-3 sec^-1)

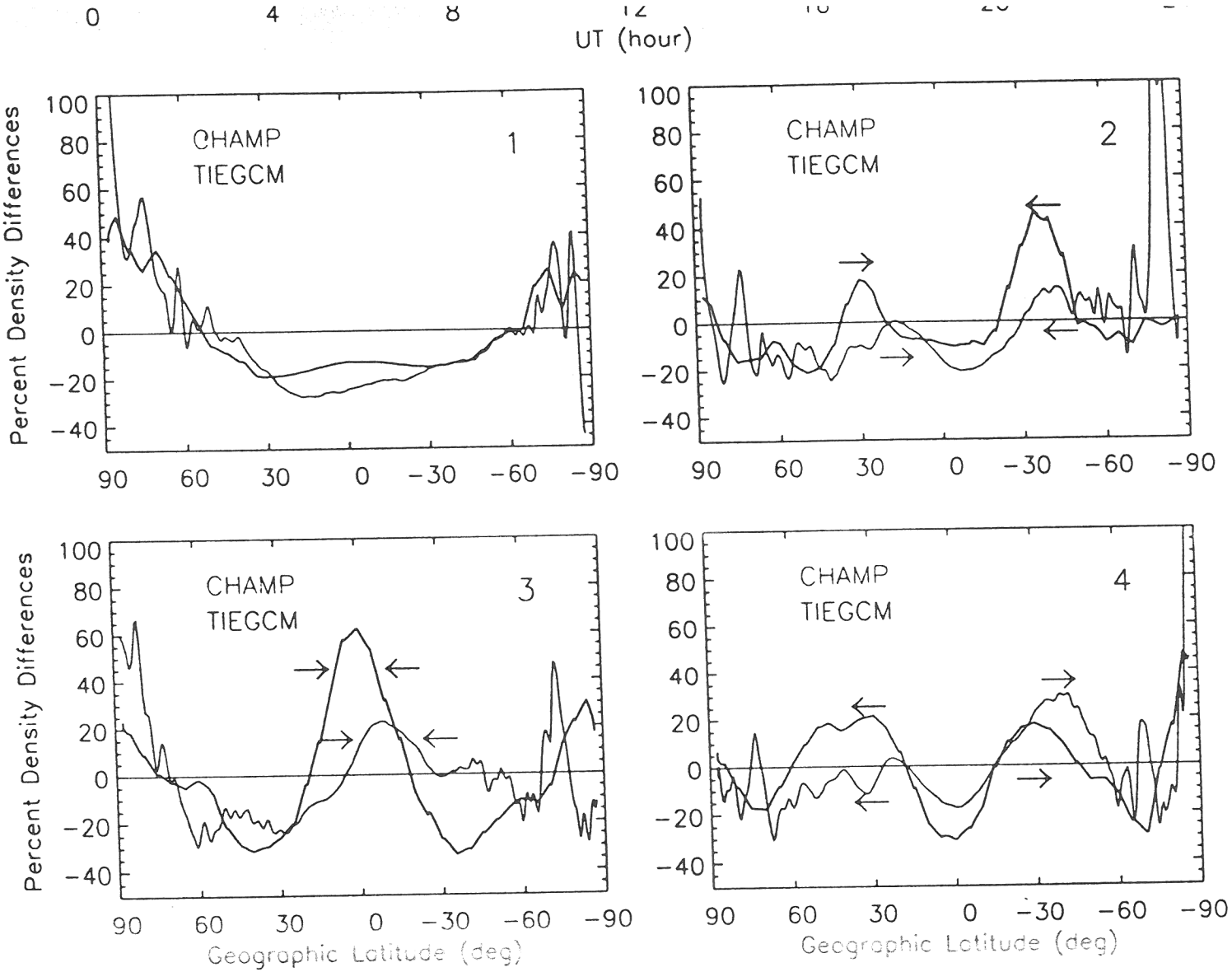

Figure 4. Comparison of CHAMP and TIEGCM nighttime densities during a magnetically disturbed period on 19 April 2002. The arrows indicate the direction of phase propagation based on the TIEGCM results. Orbit 1 is predisturbance. In orbit 2, we see large-scale density disturbances ("traveling atmospheric disturbances" or TADs) traveling through middle latitudes in both hemispheres, after being launched in their respective auroral regions. In orbit 3, the waves constructively interfere at the equator and middle latitudes, pass through each other, and on orbit 4 the TADs are passing into the opposite hemisphere.

poster

másolat Eredetileg közölte 2006 szept. amit EGU 2006-on Bencze kitett

befejezetlen

COUPLING BETWEEN THE NEUTRAL UPPER ATMOSPHERE, IONOSPHERE AND INNER MAGNETOSPHERE

P. Bencze[1], E. Illés-Almár[2], J. Verő[1]

(1) Geodetic and Geophysical Research Institute, Hungarian Academy of Sciences, H-9401 Sopron, P.O.B. 5. Hungary.
E-mail:bencze@ggki.hu

(2) Konkoly Observatory, Hungarian Academy of Sciences, H-1525 Budapest, P.O.B. 67. Hungary. E-mail: illés@konkoly.hu

General Assembly European Geosciences Union, Vienna, April 02-07, 2006

North-south asymmetry of neutral total density in the thermosphere, the density being higher in the northern than in the southern hemisphere mostly, in the northern winter months (20 satellites of $0.02 < e < 0.2$, incl. 5°-96°, altitude 175-420 km) **(Fig. 1).**

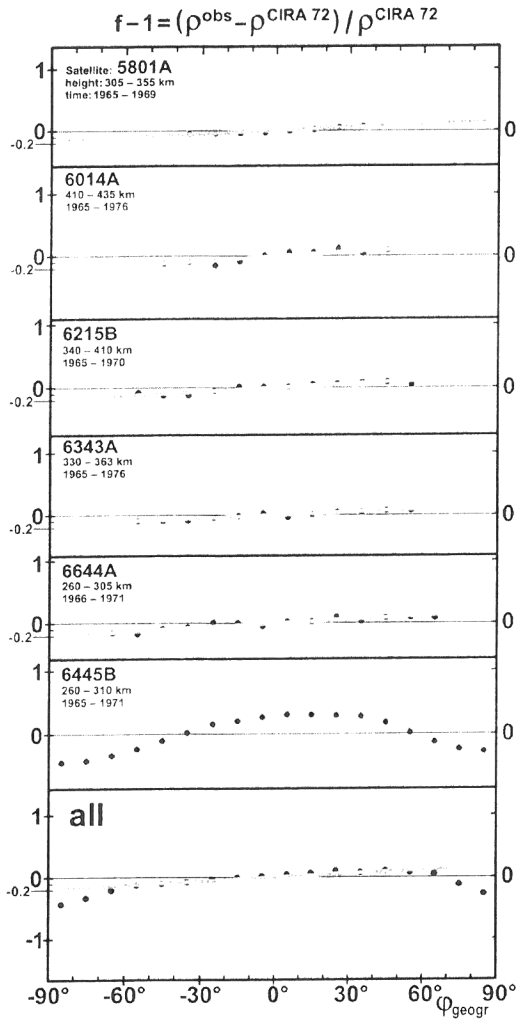

North-south asymmetry of electron density in the F-region of the ionosphere, the electron density being greater in the northern hemisphere than in the southern hemisphere mostly in the northern winter months due to enhanced neutral density representing increased atomic oxygen density and less effective β type recombination

$$(O^+ + N_z \rightarrow NO^+ + N, NO^+ + e \rightarrow N + O)$$

(Fig. 2).

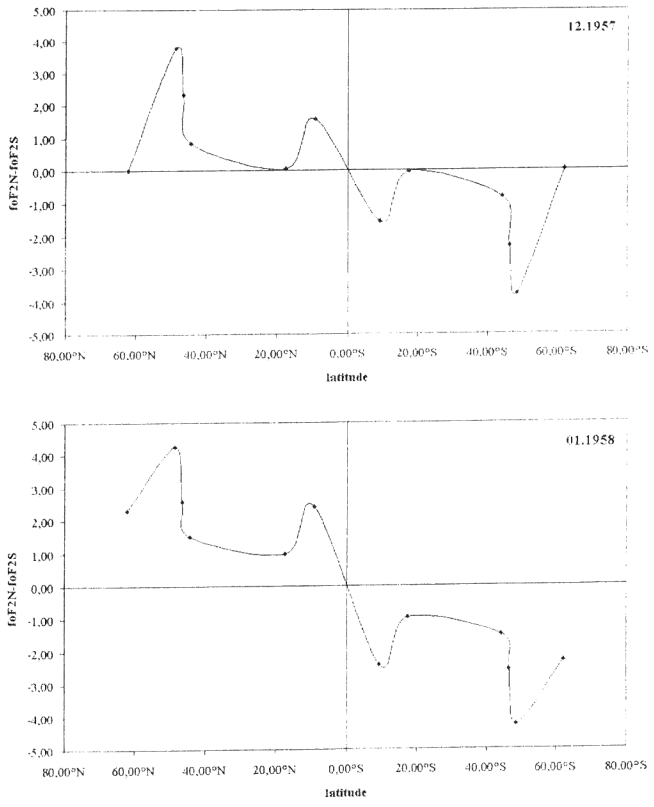

North-south asymmetry of activity and period of the FLR (**F**ield **L**ine-**R**esonance) type geomagnetic pulsations the period increasing in winter months in the northerm hemisphere related to the increased electron density $\left(T = \int(\mu_o \rho)^{1/2} ds / B\right)$ in the inner magnetosphere transferred from the ionosphere **(Fig. 3 a, b)**.

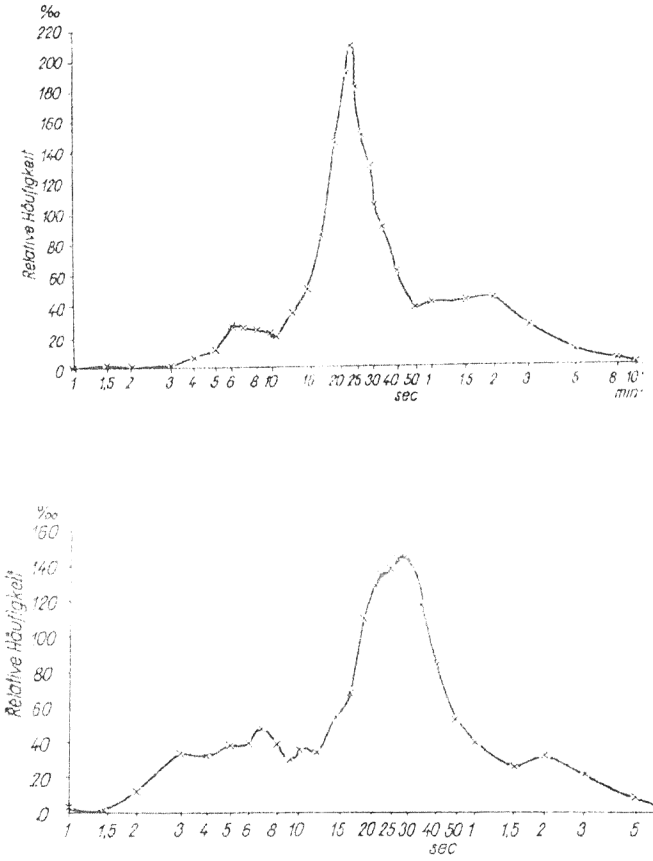

Heating in the thermosphere related to the interaction of hot ring current protons with thermal electrons, the energy conducted along geomagnetic field lines down to the ionosphere, where atomic oxygen is excited from the $O(^3P)$ to the $O(^1D)$ state and as a consequence red line emission of atomic oxygen occurs (SAR arc formation) at high mid-latitudes during geomagnetic disturbances **(Fig. 4)**.

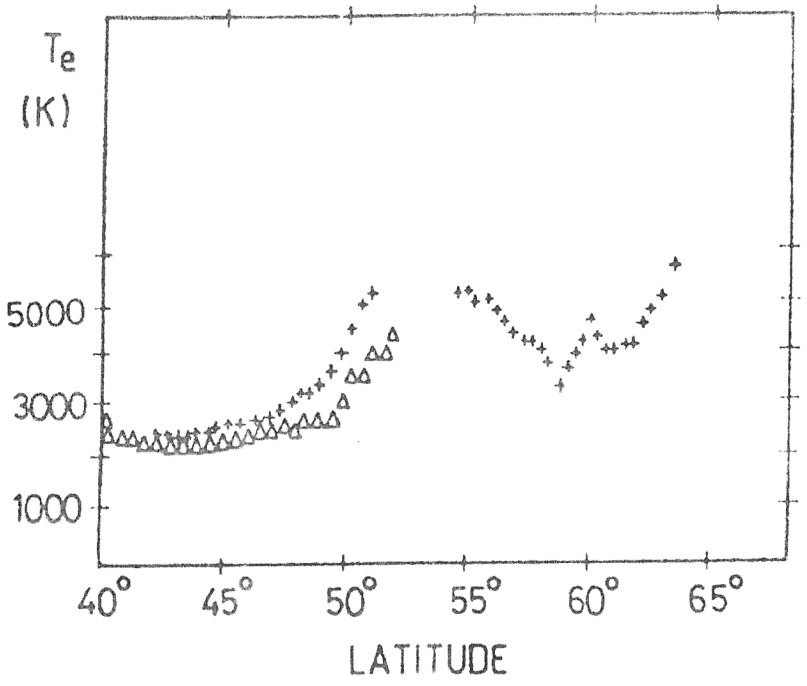

Heating in the thermosphere may be caused by protons from the inner radiation zone transferring energy by multiple charge exchange with hydrogen atoms producing energetic neutral atoms (ENA) at low mid-latitudes. As a result of this heating increased neutral density is produced **(Fig. 5)**.

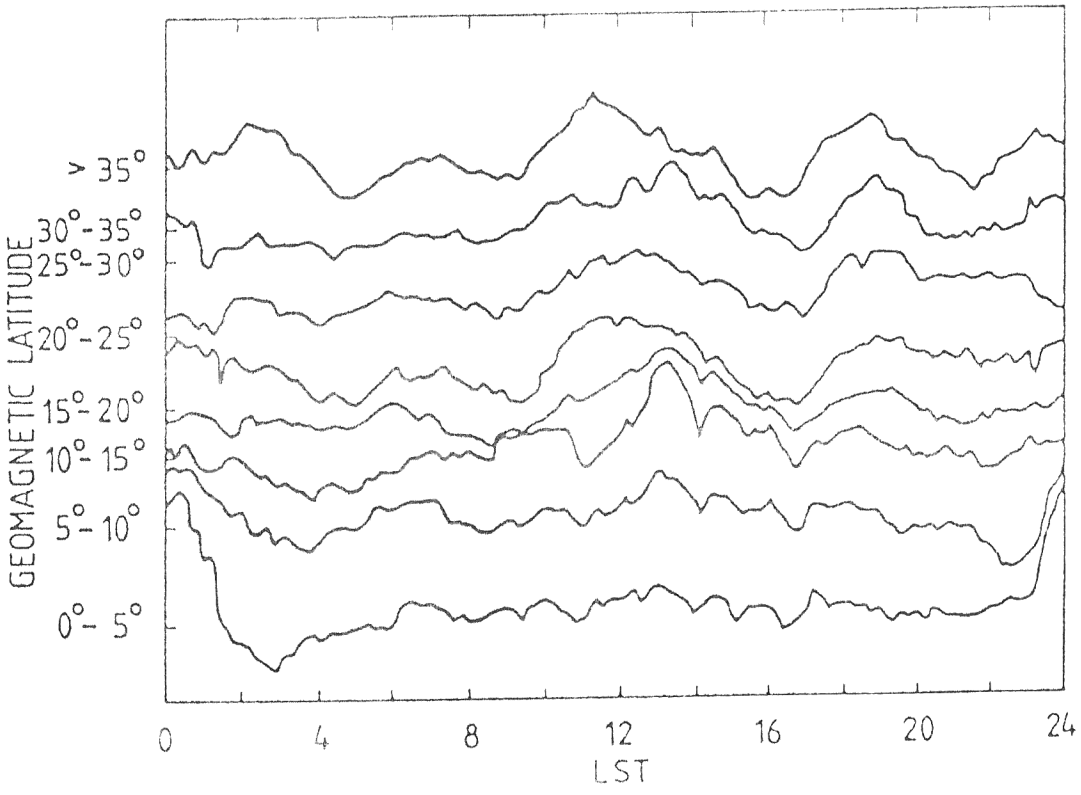

Post storm effect (geomagnetic after effect) has been observed in the lower ionosphere due to precipitation of electrons of energy > 40 keV originating in the „slot" region of the radiation belts (L ~ 3). Electron precipitation is caused by pitch angle diffusion of electrons into the loss cone related to wave-particle interaction (cyclotron resonance), in course of which particle acceleration occurs due to violation of the integral adiabatic invariant of the magnetic field **(Fig. 6)**.

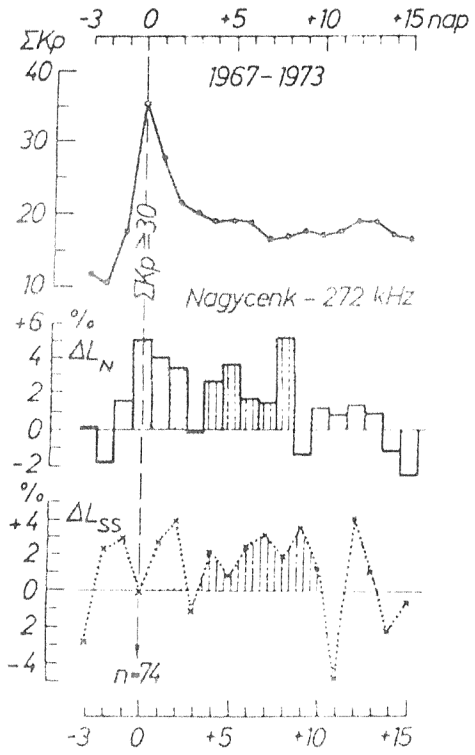

North-south asymmetry of activity and period of the FLR (**F**ield **L**ine-**R**esonance) type geomagnetic pulsations the period increasing in winter months in the northerm hemisphere related to the increased electron density $\left(T = \int(\mu_o \rho)^{1/2} ds / B\right)$ in the inner magnetosphere transferred from the ionosphere (**Fig. 3 a, b**).

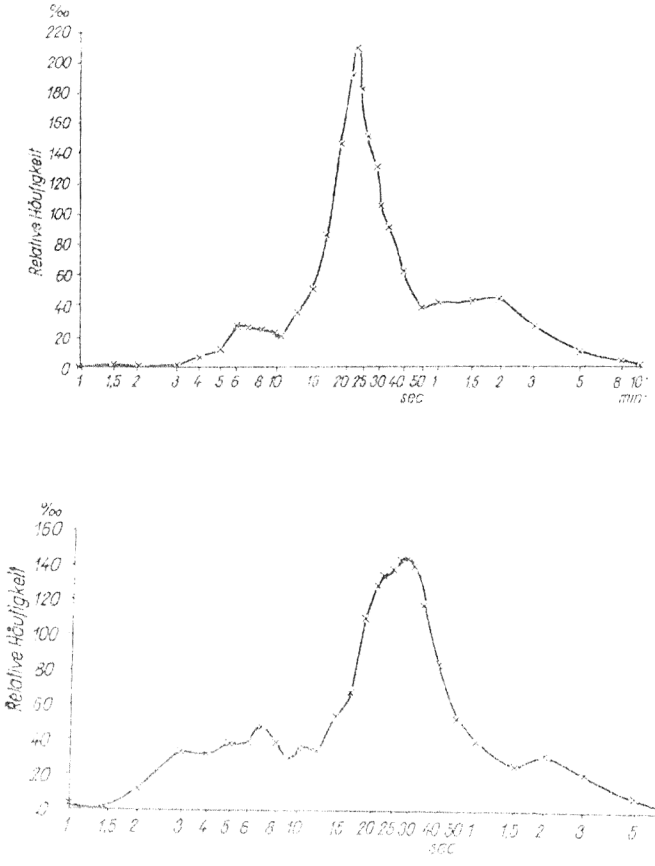

Heating in the thermosphere related to the interaction of hot ring current protons with thermal electrons, the energy conducted along geomagnetic field lines down to the ionosphere, where atomic oxygen is excited from the $O(^3P)$ to the $O(^1D)$ state and as a consequence red line emission of atomic oxygen occurs (SAR arc formation) at high mid-latitudes during geomagnetic disturbances **(Fig. 4)**.